Catal Lett
DOI 10.1007/s10562-016-1896-1

# Immobilized Sandwich-Type Polyoxometalates $[Mn_4(XW_9O_{34})_2]^{n-}$ on Tb-Doped $TiO_2$ Nanoparticles as Efficient and Selective Catalysts in the Oxidation of Sulfides and Alcohols

**Sahar Gholamyan[1] · Roushan Khoshnavazi[1] · Amin Rostami[1] · Leila Bahrami[1]**

Received: 11 June 2016 / Accepted: 25 October 2016


**Abstract** Sandwich-type polyoxometalates of $[M_4(XW_9O_{34})_2]^{n-}$ ($M = Mn^{2+}$, $Cu^{2+}$, $Zn^{2+}$, $X = Ge^{4+}$, $P^{5+}$, $As^{5+}$) supported on Ln-doped $TiO_2$ ($Ln = Nd^{3+}$, $Sm^{3+}$, $Tb^{3+}$ and $Dy^{3+}$) nanoparticles were prepared and their catalytic activities examined for oxidation of sulfides and alcohols. Results show that the catalytic activities of new nanocomposites were significantly higher than homogeneous conditions with corresponding sandwich-type polyoxometalates. The best results obtained by $[Mn_4(XW_9O_{34})_2]^{10-}$ ($X = P^{5+}$, $As^{5+}$) supported on $Tb/TiO_2$ which were characterized by various techniques. The catalysts can be easily recovered and reused for at least five times without obvious decrease of catalytic activities and the structures of the catalysts remain unchanged after recycling and the yields for catalyst recovery are all above 95%.

**Graphical Abstract**

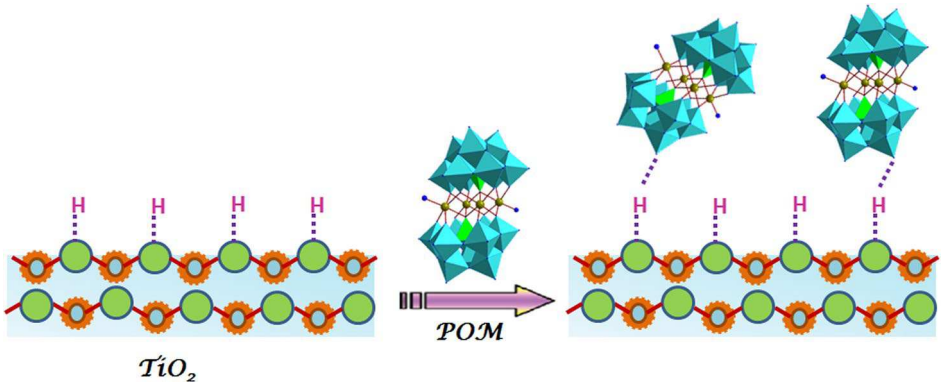


**Keywords** Sandwich-type polyoxometalates · Support · Ln-doped $TiO_2$ · Nanocomposite · Homogeneous catalyst · Hydrogen peroxide · Oxidation · Sulfides · Alcohols

**Electronic supplementary material** The online version of this article (doi:10.1007/s10562-016-1896-1) contains supplementary material, which is available to authorized users.

✉ Roushan Khoshnavazi
r.khoshnavazi@uok.ac.ir; khoshnavazi@yahoo.com

Sahar Gholamyan
gholamyansahar@yahoo.com

Amin Rostami
A.rostami@uok.ac.ir

[1] Department of Chemistry, University of Kurdistan, P.O. Box 66135-416, Sanandaj, Iran

## 1 Introduction

Polyoxometalates (POMs) are a class of nano-sized inorganic clusters presenting abundant potential in the fields of chemistry [1]. Over the last decades catalytic properties of Keggin and Dawson-type POMs were one of the most important researches topics [2, 3]. Sandwich-type POMs

due to the presence of multi metal ions in their structures are of most interest. Recently, catalytic application studies of sandwich-type POMs in which three or four metal ions located between two Keggin or Dawson moieties have been more attractive [4–7]. Although, these efforts have led to significant progress in the field of catalyst, the reported based POMs catalytic systems show the following disadvantages: (1) the recovery and reuse of the used catalysts are difficult due to their homogeneous nature; (2) the catalytic efficiency and the yields are not satisfactory in most cases for the heterogeneous catalytic systems [8]; (3) the bulk of POMs display no characteristic porosity and have low surface area. One of the most promising solutions to these problems seems to be immobilization of POMs onto solid support such as silica [9], titanium dioxide [10], zeolite [11], alumina [12]. Nanometal oxides have drawn the researcher's attention due to their unusual physical and chemical catalytic properties [13–15] and are proved to be promising catalysts because of their high activity, non-toxicity, ease of availability, reusability, strong oxidizing power, and long-term stability [16–19].

Oxidation catalysis by POMs has received much attention because their chemical properties can finely be tuned by choosing constituent elements and counter cations, and are thermally and oxidatively stable in comparison with organometallic complexes, organocatalysts, and enzymes [20–24]. Oxidation of sulfides to the corresponding sulfoxides or sulfones is an important type of organic reaction since it is closely related to the petroleum industry, which is known as oxidative desulfurization [25–31]. Sulfones and sulfoxides are important intermediates in the synthesis of many interesting biologically active compounds [32–36]. Therefore the oxidation of sulfides to sulfoxides or sulfones has been the subject of many studies and a large number of synthetic procedures are now available [16, 37–45]. The selective oxidation of primary and secondary alcohols to the corresponding carbonyl compounds is a fundamental preparative reaction, which has been widely investigated [46, 47]. A variety of different catalytic systems for hydrogen peroxide promoted oxidation of alcohols have been developed e.g. tungsten based polyoxometalate catalysts [48–53].

The use of 'green oxidants' such as hydrogen peroxide is attractive, since it is readily available, low cost, and eco-friendly, with formation of water as the only by-product [54, 55]. However, its poor oxidizing power is a main drawback, which needs catalyst for the activation of $H_2O_2$. To date, various kinds of POMs have been developed for the $H_2O_2$ and $O_2$ based green oxidations [20–24].

In comparison with the Keggin and Dawson-type POMs, the catalytic properties of sandwich-type POMs as heterogeneous catalyst have not been extensively studied [4–7]. In this work, new nanocomposites consist of sandwich-type polyoxometalates $[M_4(XW_9O_{34})_2]^{n-}$ ($M = Mn^{2+}$, $Cu^{2+}$, $Zn^{2+}$, $X = Ge^{4+}$, $P^{5+}$, $As^{5+}$) on Ln-doped $TiO_2$ ($Ln = Nd^{3+}$, $Sm^{3+}$, $Tb^{3+}$ and $Dy^{3+}$) nanoparticles (POMs/Ln/$TiO_2$) were prepared and their catalytic behaviors were examined in oxidation of sulfide and alcohols using $H_2O_2$ as oxidant. The $[M_4(XW_9O_{34})_2]^{n-}$ POMs are belonged to the B-type sandwich polyoxometalates which their structure consist of two laconary B–α-$[(XW_9O_{34})_2]^{n-}$ Keggin moieties linked via a rhomblike $M_4O_{l6}$ group leading to a $C_{2h}$ symmetry sandwich-type complex (Fig. S1) [4, 5].

## 2 Experimental

### 2.1 General

All reagents were commercially obtained and used as received. Titanium(IV) isopropoxide (TTIP) and absolute ethanol were obtained from Acrōs Organics. The lanthanides salts of $LnCl_3.6H_2O$ were obtained from Alfa Aesar. Potassium salts of $[M_4(XW_9O_{34})_2]^{n-}$ ($M = Mn^{2+}$, $Cu^{2+}$, $Zn^{2+}$, $X = Ge^{4+}$, $P^{5+}$, $As^{5+}$) were prepared according to the previously reported method [56, 57]. X-ray diffraction (XRD) patterns were recorded with an X'PertPro Analytical, Holland diffractometer (Model PW1840) in 40 kV and 30 mA with a CuKα radiation (λ = 1.5418 A). FT-IR spectra were obtained using a Bruker Vector 22 FT-IR spectrometer using KBr pellet. Scanning electron micrographs (SEM) and energy-dispersive X-ray (EDX) analysis of the samples were taken with FESEM-TESCAN MIRA3. The X-ray photoelectron (XPS) spectra of the supported catalyst was recorded on a VG Microtech Twin anode XR3E2 X-ray source and aconcentric hemispherical analyzer operated at a base pressure of $5 \times 10^{-10}$ mbar using AlKa (hm = 1486.6 eV). Peak fitting of all spectra were performed using the Shirley background correction and Gaussian–Lorentzian peak shapes. Binding energies (BEs) were referenced to C 1 s peak at 284.5 eV. Low-resolution survey spectra, as well as higher-resolution spectra for W, Mn, O, As and Ti were collected.

### 2.2 Methods

#### *2.2.1 Preparation of Ln/$TiO_2$ Nano-Sized*

The support was synthesized using reported procedure [58]. 10 mL of $Ti\{OCH(CH_3)_2\}_4$ is added at room temperature to 30 mL of EtOH. The pH of mixture is adjusted to 1.5 by concentrated hydrochloric acid (solution 1). $LnCl_3.6H_2O$ (0.2 mmol), the rare earth precursor, was dissolved into the solution containing $H_2O$ (2 mL) and EtOH (4 mL) (solution 2). Then, solution 2 was added

dropwise into solution 1 during 10 min approximately. The resulting acidic mixture was stirred constantly for about 3 h until sol was obtained. The sol was maintained for 24 h till gel formation. The gel was dried at 373 K for 4 h and then calcined at 823 K for 3 h. The rare earth doping in the support is 1.0%. Pure $TiO_2$ powder was also prepared by the same process without doping [58].

#### 2.2.2 Preparations of Catalyst Nanocomposites

The impregnation process is as following: 1.00 g of $Ln/TiO_2$ support was dispersed in water solution containing a given amount of (10, 20 and 30% w/w) of $[M_4(XW_9O_{34})_2]^{n-}$ ($M = Mn^{2+}$, $Cu^{2+}$, $Zn^{2+}$, $X = Ge^{4+}$, $P^{5+}$, $As^{5+}$). The suspension was stirred continuously under room temperature. After 24 h, water was removed by evaporation at 373 K. The final product was obtained by drying at 373 K for 2 h. The loading levels of $[M_4(XW_9O_{34})_2]^{n-}$ in prepared composites by mass are 10, 20 and 30%.

#### 2.2.3 General Procedure for the Oxidation of Sulfides to Sulfoxides

A mixture of $[Mn_4(AsW_9O_{34})_2]^{10-}/Tb/TiO_2$ (50 mg), sulfide (1 mmol), 30% $H_2O_2$ aqueous solution (6 mmol), acetonitrile (3 mL) was stirred at room temperature for the time specified (Table 2). After the completion of the reaction, which was monitored by TLC (EtOAc/*n*-Hexane, 4/10), the water (5 mL) was added and catalyst was centrifuged. The product was extracted with $CH_2Cl_2$ (3 × 5 mL) and the combined organic extractions washed with brine (10 mL) and dried over anhydrous $Na_2SO_4$. The solvent was evaporated under reduced pressure to give the corresponding pure sulfoxide in most cases.

#### 2.2.4 General Procedure for the Oxidation of Sulfides to Sulfones

A mixture of $[Mn_4(PW_9O_{34})_2]^{10-}/Tb/TiO_2$ (50 mg), sulfide (1 mmol), 30% $H_2O_2$ aqueous solution (6 mmol) and acetonitrile (3 mL) was stirred at room temperature for the time specified (Table 2). After the completion of the reaction, which was monitored by TLC (EtOAc/*n*-Hexane, 4/10), the water (5 mL) was added and catalyst was centrifuged. The product was extracted with $CH_2Cl_2$ (3 × 5 mL) and the combined organic extractions washed with brine (10 mL) and dried over anhydrous $Na_2SO_4$. Evaporation of the solvent under reduced pressure gives the pure corresponding sulfone in most cases.

#### 2.2.5 General Procedure for the Oxidation of Benzylic Alcohols

A mixture of $[Mn_4(PW_9O_{34})_2]^{10-}/Tb/TiO_2$ (40 mg), alcohols (1 mmol), 30% $H_2O_2$ aqueous solution (6 mmol) and $H_2O$ (1 mL) was stirred at 80 °C for the time specified (Table 4). After the completion of the reaction, which was monitored by TLC (EtOAc/*n*-Hexane, 4/10), the catalyst was centrifuged. The product was extracted with $CH_2Cl_2$ (3 × 5 mL) and the combined organic extractions washed with brine (10 mL) and dried over anhydrous $Na_2SO_4$. The solvent was removed under reduced pressure to give the corresponding pure carbonyl compound in most cases.

## 3 Results and Discussion

### 3.1 Preparation of POMs/Ln/$TiO_2$ Nanocomposites

$TiO_2$ and $Ln/TiO_2$ support, was synthesized via sol–gel technique and nanocomposites were prepared by impregnation method [58]. In next step, $[M_4(XW_9O_{34})_2]^{n-}$ ($M = Mn^{2+}$, $Cu^{2+}$, $Zn^{2+}$, $X = Ge^{4+}$, $P^{5+}$, $As^{5+}$) were supported on $Ln/TiO_2$ ($Ln = Nd^{3+}$, $Sm^{3+}$, $Tb^{3+}$ and $Dy^{3+}$) nanoparticles and their catalytic behaviors were evaluated.

The surface of $Ln/TiO_2$ particles is positively charged in acidic media, whereas the POMs are negatively charged, thus facilitating the adsorption of the POMs species on the surface of $TiO_2$ particles by simple coulombic interactions. Yoon and co-workers have demonstrated that there are three different hydrogen bonds between POMs and $TiO_2$ colloidal particles in aqueous solution, i.e., =Ti–OH...$O_t$=W, =Ti–OH...$O_b$=W, and =Ti–OH...$O_c$=W ($O_t$ terminal oxygen, $O_{b,c}$ bridge oxygen), on the basis of infrared spectral analysis. Almost all the added POMs were completely adsorbed on $TiO_2$ [59].

### 3.2 Characterization of POMs/Tb/$TiO_2$ Nanocomposites

#### 3.2.1 FT-IR Analysis

Figure 1 shows the FT-IR spectra of $Tb/TiO_2$, $[Mn_4(XW_9O_{34})_2]^{10-}$ ($X = P^{5+}$ and $As^{5+}$) and their nanocomposites with different loadings of $[Mn_4(PW_9O_{34})_2]^{10-}$ on $Tb/TiO_2$. The characteristic peaks of at 1030, 937, 880, 742 $cm^{-1}$ in $[Mn_4(PW_9O_{34})_2]^{10-}$ spectrum are attributed to $\nu_{as}$(P–$O_a$), $\nu_{as}$(W=$O_d$), $\nu_{as}$(W–$O_b$–W), $\nu_{as}$(W–$O_c$–W), respectively (Fig. 1A), and at 951, 868, 838, 730 $cm^{-1}$ in that of $[Mn_4(AsW_9O_{34})_2]^{10-}$ are attributed to $\nu_{as}$(As–$O_a$), $\nu_{as}$(W=$O_d$), $\nu_{as}$(W–$O_b$–W), $\nu_{as}$(W–$O_c$–W), respectively (Fig. 1B) [60]. From Fig. 1, it can be seen that the IR spectrum of $Tb/TiO_2$ illustrates an intense, broad, indistinct region between 1100 and 400 $cm^{-1}$. The FT-IR

spectra of POMs/Tb/$TiO_2$ show characteristic peaks of Tb/$TiO_2$ and POMs which intensities of the later increase by increasing the amounts of loading polyoxometalate on the Tb/$TiO_2$. As a result, some characteristic peaks of $[Mn_4(XW_9O_{34})_2]^{10-}$ ($X = P^{5+}$, $As^{5+}$) with that of Tb/$TiO_2$ in nanocomposites are overlapped in this area (Fig. 1). However, some vibration peaks of $[Mn_4(XW_9O_{34})_2]^{10-}$ ($X = P^{5+}$, $As^{5+}$) unit still can be seen clearly, which indicates that the $[Mn_4(XW_9O_{34})_2]^{10-}$ ($X = P^{5+}$, $As^{5+}$) structure has not been destroyed upon immobilization on Tb/$TiO_2$ nano particle [58].

For surface analysis of nanocomposite of $[Mn_4(PW_9O_{34})_2]^{10-}$/Tb/$TiO_2$ with 10 and 20% loading of $[Mn_4(PW_9O_{34})_2]^{10-}$, Attenuated Total Reflectance Fourier Transform IR spectroscopy (ATR FT-IR) was used. The ATR FT-IR spectra of $[Mn_4(PW_9O_{34})_2]^{10-}$/Tb/$TiO_2$ with 10 and 20% loading of $[Mn_4(PW_9O_{34})_2]^{10-}$ and Tb/$TiO_2$ is given in Fig. 2. As expected, the appearance of POMs component on the surface of the prepared nanocomposites must be greater than that expected from the mass ratio. The ATR FT-IR spectrum of POMs/Tb/$TiO_2$ show characteristic peaks of Tb/$TiO_2$ and POMs which it also is an evidence for loading desired POM.

### 3.2.2 XRD Analysis

The X-ray diffraction patterns of Tb/$TiO_2$, $[Mn_4(PW_9O_{34})_2]^{10-}$/Tb/$TiO_2$ and $[Mn_4(AsW_9O_{34})_2]^{10-}$/Tb/$TiO_2$ with 20% loading levels of POMs are shown in Fig. 3. It can be observed that the XRD patterns of Tb/$TiO_2$ and $[Mn_4(PW_9O_{34})_2]^{10-}$/Tb/$TiO_2$ and $[Mn_4(AsW_9O_{34})_2]^{10-}$ are similar, in which all of them crystallized in the anatase structure. Moreover, there are no characteristic peaks of POMs and Tb-$TiO_2$ in the XRD spectrum of nanocomposites. This indicates that $Tb^{3+}$ and POM species are well-dispersed in the surface of the $TiO_2$ [61, 62].

### 3.2.3 BET Analysis

The surface area of Tb/$TiO_2$, $K_{10}[Mn_4(AsW_9O_{34})_2]\cdot xH_2O$ and $[Mn_4(AsW_9O_{34})_2]^{10-}$/Tb/$TiO_2$ with 20% loading of $[Mn_4(AsW_9O_{34})_2]^{10-}$ was analyzed by BET. The BET analysis showed that Tb/$TiO_2$ has a 74.91 $m^2/g$ surface area. This surface area is larger than that of naked $TiO_2$ [58]. The high surface area can be explained by small crystallite size and high dispersion of terbium ion in the Tb/$TiO_2$. As expected, surface area of the solid $K_{10}[Mn_4(PW_9O_{34})_2]\cdot xH_2O$ is very small (7.55 $m^2/g$). The BET analysis illustrates that surface area of the $[Mn_4(PW_9O_{34})_2]^{10-}$/Tb/$TiO_2$ with 20% loading of $[Mn_4(AsW_9O_{34})_2]^{10-}$ is 68.63 $m^2/g$. The results confirm well that the effective surface area of $K_{10}[Mn_4(PW_9O_{34})_2]\cdot xH_2O$ markedly increased by immobilization on Tb/$TiO_2$ surface.

### 3.2.4 XPS Analysis

X-ray Photoelectron Spectroscopy (XPS) is widely used to investigate the chemical composition of surfaces. XPS survey spectra of $[Mn_4(AsW_9O_{34})_2]^{10-}$/Tb/$TiO_2$ with 20%

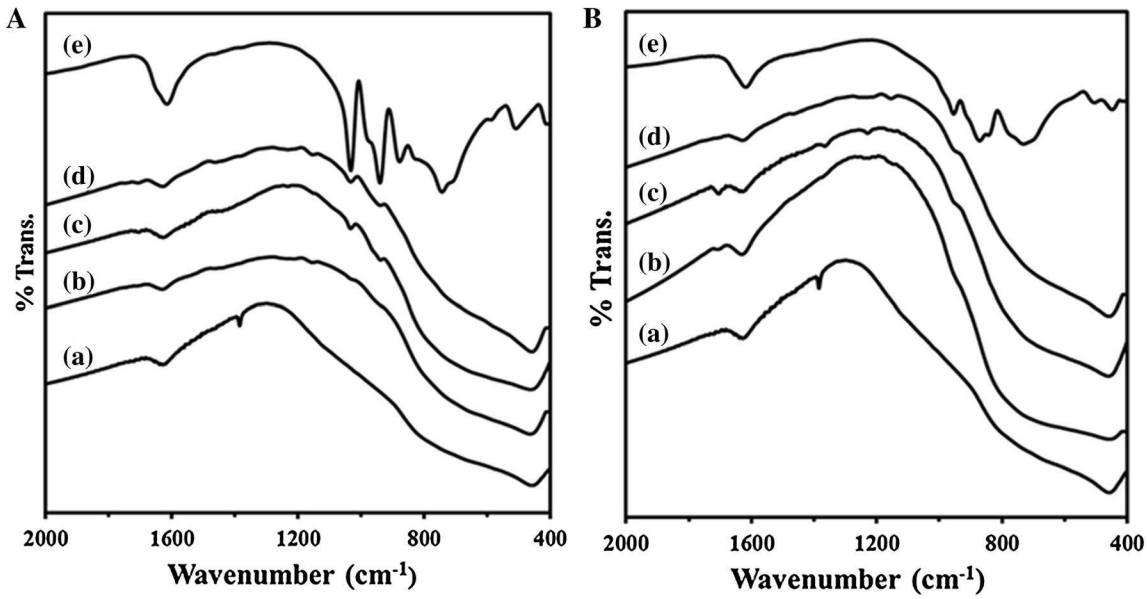


**Fig. 1** The FT-IR spectra of the prepared nanocopmposites **A** *a* Tb/$TiO_2$, *b–d* $[Mn_4(PW_9O_{34})_2]^{10-}$/Tb/$TiO_2$ with 10–30% loading of $[Mn_4(PW_9O_{34})_2]^{10-}$ respectively and *e* $[Mn_4(PW_9O_{34})_2]^{10-}$. **B** *a* Tb/$TiO_2$, *b–d* $[Mn_4(AsW_9O_{34})_2]^{10-}$/Tb/$TiO_2$ with 10–30% loading of $[Mn_4(AsW_9O_{34})_2]^{10-}$ respectively and *e* $[Mn_4(AsW_9O_{34})_2]^{10-}$

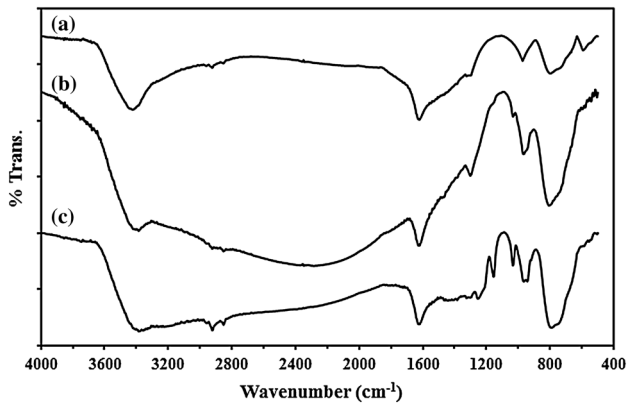


**Fig. 2** The ATR FT-IR spectra of the prepared nanocopmposites *a* $Tb/TiO_2$, *b* $[Mn_4(PW_9O_{34})_2]^{10-}/Tb/TiO_2$ with 10% loading of $[Mn_4(PW_9O_{34})_2]^{10-}$ and *c* $[Mn_4(PW_9O_{34})_2]^{10-}/Tb/TiO_2$ with 20% loading of $[Mn_4(PW_9O_{34})_2]^{10-}$

loading levels of POMs are shown in Fig. 4. As expected, Ti 2p, O 1s, C 1s, W 4f and Mn 2p peaks were seen in the XPS survey spectra. From the XPS spectrum of Ti, peaks corresponding to Ti-O are observed at 466.8 and 472 eV can be attributed to the $2p_{3/2}$ and $2p_{1/2}$ respectively. The peaks observed at 538 eV can be assigned to the binding energy of O 1s. The XPS peak for C1s (284.8 eV) is due to the adventitious hydrocarbon from the XPS instrument itself. The W 4f spectrum can be deconvoluted into doublets. This doublet consists of W $4f_{7/2}$ line at 35.3 eV and W $4f_{5/2}$ line at 37.1 eV, which are assigned to the W in the W–O bond configuration and typically observed for the $W^{6+}$ [63]. Due to very low Mn and Tb content in $[Mn_4(AsW_9O_{34})_2]^{10-}/Tb/TiO_2$ in comparison to Ti content intensity of the corresponding peaks are low. The low intensity peaks at 640 and 650 eV may be attributed to the Mn $2p_{3/2}$ and Mn $2p_{1/2}$, respectively [64].

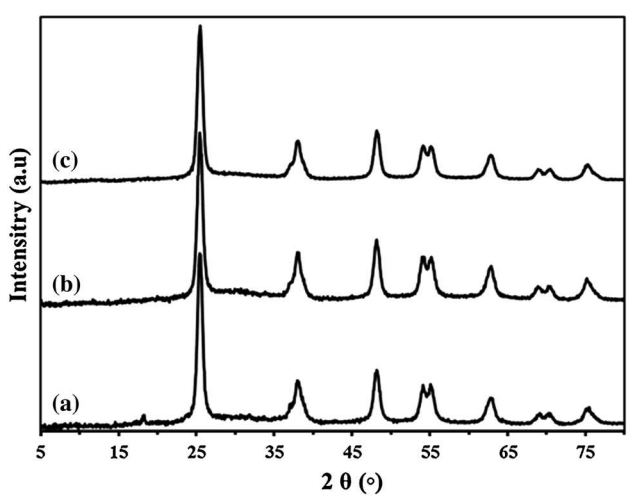


**Fig. 3** XRD patterns of *a* $Tb/TiO_2$, *b* $[Mn_4(PW_9O_{34})_2]^{10-}/Tb/TiO_2$ with 20% loading of $[Mn_4(PW_9O_{34})_2]^{10-}$ and *c* $[Mn_4(AsPW_9O_{34})_2]^{10-}/Tb/TiO_2$ with 20% loading of $[Mn_4(AsPW_9O_{34})_2]^{10-}$

### *3.2.5 SEM Images*

The SEM images of the nanocomposite of $[Mn_4(AsW_9O_{34})_2]^{10-}/Tb/TiO_2$ with 10% loading level of POMs (Fig. 5) reveal that nanocomposite remain relatively uniform regular spherical with particles diameter less than 20 nm.

### *3.2.6 EDX Spectra*

In order to achieve information about the elemental composition and distribution on the surface of the sample of $[Mn_4(PW_9O_{34})_2]^{10-}/Tb/TiO_2$ with 10% loading level was characterized by using energy dispersive X-ray analysis (EDX). EDX analysis detects the presence of Mn, O, As, Tb, W elements (Fig. 6). Based on the above results, it is demonstrated that of $[Mn_4(AsW_9O_{34})_2]^{10-}$ was immobilized onto the surface of the $Tb/TiO_2$ nanoparticles.

## 4 Catalytic Application of POMs/Ln/$TiO_2$

### 4.1 Catalytic Application of POMs/Ln/$TiO_2$ in the Oxidation of Sulfides to Sulfoxides and Sulfones

The catalytic application of the sandwich-type polyoxometalates $[M_4(XW_9O_{34})_2]^{n-}$ ($M = Mn^{2+}$, $Cu^{2+}$, $Zn^{2+}$; $X = Ge^{4+}$, $P^{5+}$, $As^{5+}$) on Ln/doped $TiO_2$ ($Ln = Nd^{3+}$, $Sm^{3+}$, $Tb^{3+}$, $Dy^{3+}$) nanoparticles in the oxidation of sulfide using $H_2O_2$ as oxidant was investigated. Initially, in order to investigation of catalyst effect, the oxidation of methyl

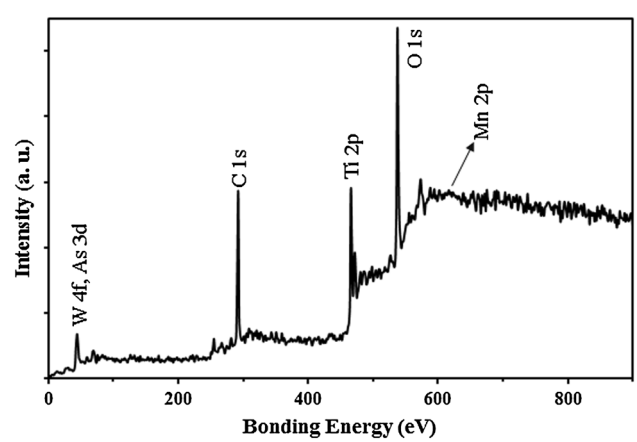


**Fig. 4** XPS survey spectra of $[Mn_4(AsW_9O_{34})_2]^{10-}/Tb/TiO_2$ with 20% loading of $[Mn_4(AsW_9O_{34})_2]^{10-}$

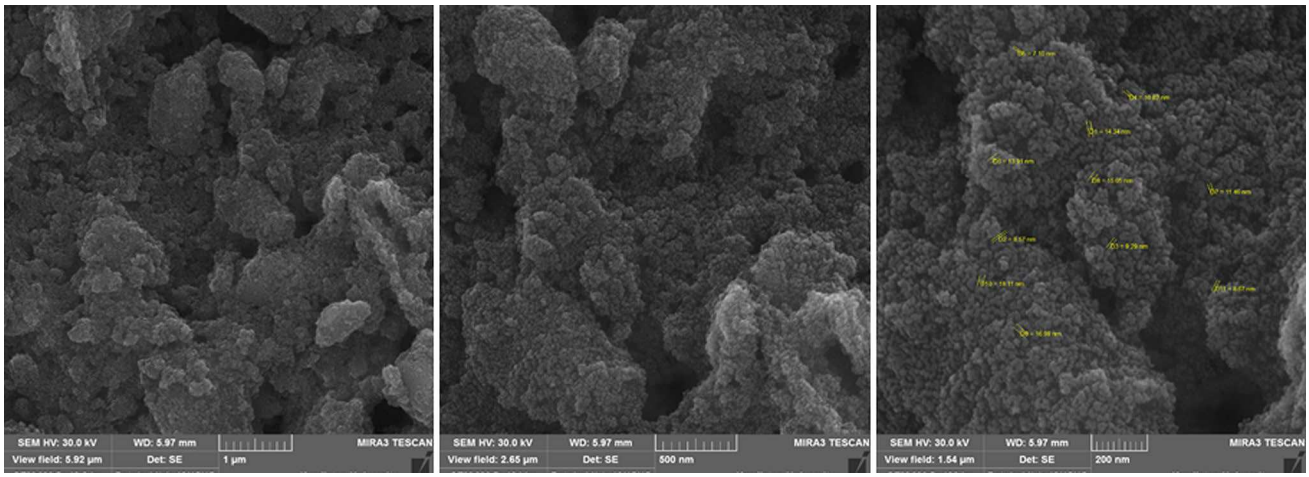


**Fig. 5** SEM images of $[Mn_4(AsW_9O_{34})_2]^{10-}/Tb/TiO_2$ with 10% loading of $[Mn_4(AsW_9O_{34})_2]^{10-}$

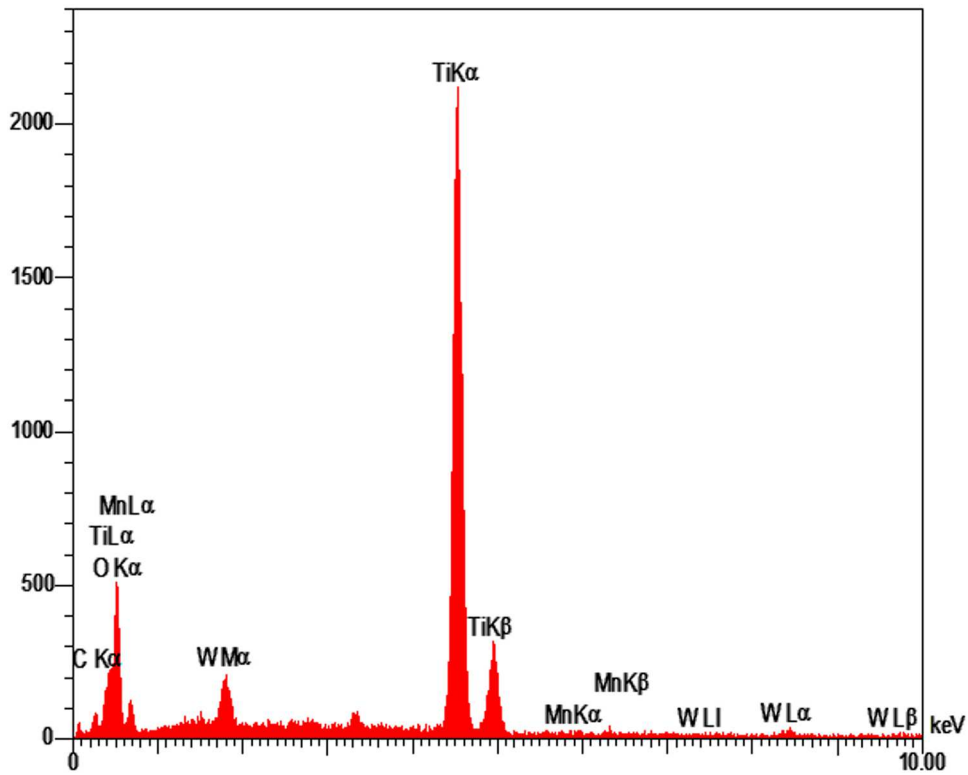


**Fig. 6** The EDX spectra of $[Mn_4(AsW_9O_{34})_2]^{10-}/Tb/TiO_2$ with 10% loading of $[Mn_4(AsW_9O_{34})_2]^{10-}$

phenyl sulfide (as model reaction) was performed using hydrogen peroxide in the presence of various catalysts in $CH_3CN$ at room temperature (Table 1). The reaction was incomplete in the absence of any catalyst and in the presence of $TiO_2$, $Tb/TiO_2$ and $[M_4(XW_9O_{34})_2]^{10-}$ ($X = P^{5+}$, $As^{5+}$; $M = Cu^{2+}$, $Zn^{2+}$) (Table 1, entries 1–4). No product was obtained by using of homogeneous sandwich-type polyoxometalate $[Mn_4(GeW_9O_{34})_2]^{12-}$ (Table 1, entry 5). Using $[Mn_4(AsW_9O_{34})_2]^{10-}/Tb/TiO_2$ as nanocatalyst gave the complete conversion of methyl phenyl sulfide to methyl phenyl sulfoxide by surprisingly high chemo selectivity in very short reaction time in $CH_3CN$ at room temperature (Table 1, entry 6). Under the same reaction conditions, only sulfone was obtained in the presence of $[Mn_4(PW_9O_{34})_2]^{10-}/Tb/TiO_2$ as catalyst (Table 1, entry 7). Nanocomposites of $[M_4(PW_9O_{34})_2]^{n-}/Tb/TiO_2$ ($M = Cu^{2+}$, $Zn^{2+}$) and $[M_4(AsW_9O_{34})_2]^{10-}/Tb/TiO_2$ ($M = Cu^{2+}$, $Zn^{2+}$) give relatively low yields of sulfones and sulfoxides, respectively (Table 1, entries 8–11). Other nanocomposites such as $[Mn_4(GeW_9O_{34})_2]^{12-}/Tb/TiO_2$ is not effective

**Table 1** Investigate effect of catalysts on the oxidation of methyl phenyl sulfide to methyl phenyl sulfoxide or to methyl phenyl sulfone with $H_2O_2$ as oxidant

| Entry | Catalyst (50 mg) | Solvent | Time (min) | Sulfoxide (%)[a,b] | Sulfone (%)[a,b] |
|---|---|---|---|---|---|
| 1 | Catalyst-free | $CH_3CN$ | 2880 | 50 | – |
| 2 | $TiO_2$ | $CH_3CN$ | 2880 | 25 | 25 |
| 3 | $Tb/TiO_2$ | $CH_3CN$ | 2880 | 25 | 25 |
| 4 | $[M_4(XW_9O_{34})_2]^{10-}$ M = Mn,Cu, Zn X = P, As | $CH_3CN$ | 900 | 25 | – |
| 5 | $[M_4(XW_9O_{34})_2]^{12-}$ M = Mn, Cu, Zn X = Ge | $CH_3CN$ | 2880 | – | – |
| 6 | $[Mn_4(AsW_9O_{34})_2]^{10-}/Tb/TiO_2$ (10%) | $CH_3CN$ | 2 | 100 | – |
| 7 | $[Mn_4(PW_9O_{34})_2]^{10-}/Tb/TiO_2$ (10%) | $CH_3CN$ | 2 | – | 100 |
| 8 | $[Cu_4(AsW_9O_{34})_2]^{10-}/Tb/TiO_2$ (10%) | $CH_3CN$ | 120 | 70 | – |
| 9 | $[Zn_4(AsW_9O_{34})_2]^{10-}/Tb/TiO_2$ (10%) | $CH_3CN$ | 120 | 70 | – |
| 10 | $[Cu_4(PW_9O_{34})_2]^{10-}/Tb/TiO_2$ (10%) | $CH_3CN$ | 120 | – | 70 |
| 11 | $[Zn_4(PW_9O_{34})_2]^{10-}/Tb/TiO_2$ (10%) | $CH_3CN$ | 120 | – | 70 |
| 12 | $[Mn_4(GeW_9O_{34})_2]^{10-}/Tb/TiO_2$ (10%) | $CH_3CN$ | 600 | 20 | Trace |
| 13 | $[Mn_4(PW_9O_{34})_2]^{10-}/TiO_2$ (10%) | $CH_3CN$ | 15 | 50 | 50 |
| 14 | $[Mn_4(AsW_9O_{34})_2]^{10-}/Nd/TiO_2$ (10%) | $CH_3CN$ | 15 | 100 | – |
| 15 | $[Mn_4(AsW_9O_{34})_2]^{10-}/Sm/TiO_2$ (10%) | $CH_3CN$ | 15 | 100 | – |
| 16 | $[Mn_4(PW_9O_{34})_2]^{10-}/Nd/TiO_2$(10%) | $CH_3CN$ | 15 | – | 100 |
| 17 | $[Mn_4(PW_9O_{34})_2]^{10-}/Sm/TiO_2$(10%) | $CH_3CN$ | 15 | – | 100 |
| 18 | $[Mn_4(AsW_9O_{34})_2]^{10-}/Dy/TiO_2$ (10%) | $CH_3CN$ | 120 | 25 | 25 |
| 19 | $[Mn_4(PW_9O_{34})_2]^{10-}/Dy/TiO_2$ (10%) | $CH_3CN$ | 120 | 25 | 25 |
| 20 | $[Mn_4(AsW_9O_{34})_2]^{10-}/Tb/TiO_2$ (5%) | $CH_3CN$ | 12 | 100 | – |
| 21 | $[Mn_4(PW_9O_{34})_2]^{10-}/Tb/TiO_2$ (5%) | $CH_3CN$ | 12 | – | 100 |
| 22 | $[Mn_4(AsW_9O_{34})_2]^{10-}/Tb/TiO_2$ (20%) | $CH_3CN$ | 2 | 100 | – |
| 23 | $[Mn_4(PW_9O_{34})_2]^{10-}/Tb/TiO_2$ (20%) | $CH_3CN$ | 2 | – | 100 |

[a]Conversions determined by GC

[b]Reaction conditions for the selective oxidation of sulfides to sulfoxides/sulfones: methyl phenyl sulfide (1 mmol), 30% $H_2O_2$ aqueous solution (6 mmol), acetonitrile (3 mL) at room temperature

**Table 2** Selective oxidation of sulfides to sulfones or sulfoxides with hydrogen peroxide catalyzed by $[Mn_4(PW_9O_{34})_2]^{10-}/Tb/TiO_2$ and $[Mn_4(AsW_9O_{34})_2]^{10-}/Tb/TiO_2$ respectively

| Entry | Substrate | Sulfoxide[a, b] | | Sulfone[a, b] | |
|---|---|---|---|---|---|
| | | Time (min) | Yield (%) | Time (min) | Yield (%) |
| 1 | 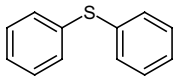 | 50 | 80 | 55 | 90 |
| 2 | 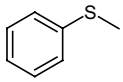 | 2 | 100 | 2 | 100 |
| 3 | 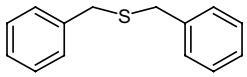 | 2 | 90 | 2 | 90 |
| 4 | 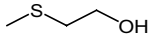 | 10 | 80 | 15 | 80 |
| 5 | 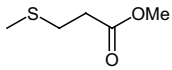 | 15 | 90 | 25 | 90 |
| 6 | 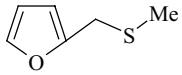 | 15 | 90 | 25 | 90 |

[a]All the products are known and were characterized by IR and [1]HNMR and by melting point comparison with those of authentic samples [65, 66]

[b]Reaction conditions for the selective oxidation of sulfides to sulfoxides/sulfones: sulfides (1 mmol), 30% $H_2O_2$ aqueous solution (6 mmol), acetonitrile (3 mL) at room temperature

(Table 1, entry 12). Nanocomposite of $[Mn_4(PW_9O_{34})_2]^{10-}/TiO_2$ (without Tb metal) is not able to produce selective product and give the mixture sulfoxide and sulfone (Table 1, entry 13). When $[Mn_4(PW_9O_{34})_2]^{10-}/TiO_2$ was doped with lanthanide metals like samarium and neodymium, the reactions were performed in the longer times (Table 1, entries 14–17) and changing the metal to Dysprosium was not effective for the reaction (Table 1, entries 18 and 19).

The effect of different loadings of $[Mn_4(XW_9O_{34})_2]^{n-}$ ($X = P^{5+}$, $As^{5+}$) in oxidation of methyl phenyl sulfide under the same reaction conditions was also investigated. A 10% loading of $[Mn_4(XW_9O_{34})_2]^{n-}$ ($X = P^{5+}$, $As^{5+}$) need for the complete conversion of methyl phenyl sulfide to methyl phenyl sulfoxide or sulfone. With 5% loading of $[Mn_4(XW_9O_{34})_2]^{n-}$ ($X = P^{5+}$, $As^{5+}$), reactions were performed in the longer times (Table 1, entries 20 and 21) and when 20% loading of $[Mn_4(XW_9O_{34})_2]^{n-}$ ($X = P^{5+}$, $As^{5+}$) was used no significant changes in the catalytic properties of nanocomposite was observed (Table 1, entries 22 and 23). The results indicate that the best loading level is 10%, which is also the saturation value of loading level. At loading levels 20% and higher, the excess POMs is easy to drop from the composite during the reaction [58].

In order to generalize the scope of the reaction, various aromatic and aliphatic sulfides were subjected to oxidation using hydrogen peroxide in the presence of the catalytic amount of $[Mn_4(PW_9O_{34})_2]^{10-}/Tb/TiO_2$ and $[Mn_4(AsW_9O_{34})_2]^{10-}/Tb/TiO_2$ in $CH_3CN$ at room temperature. We have found that the expected products were obtained with high yields in short reaction times (Table 2). Interestingly, oxidation of methyl 2-hydroxyethyl sulfide proceeded chemo selectively without oxidation of the hydroxyl group (Table 2, entry 4).

### 4.2 Catalytic Application of POMs/Tb/$TiO_2$ in Oxidation of Benzylic Alcohols

In this work, the sandwich-type polyoxometalates $[M_4(XW_9O_{34})_2]^{n-}$ ($M = Mn^{2+}$, $Cu^{2+}$, $Zn^{2+}$, $X = Ge^{4+}$, $P^{5+}$, $As^{5+}$) on Tb-doped $TiO_2$ nanoparticles catalysts were used for the oxidation of benzylic alcohols using hydrogen peroxide. The oxidation of benzyl alcohol was selected as the model reaction and the effect of various catalysts were investigated in water at 80 °C (Table 3). The reaction was failed in the absence of any catalyst and in the presence of $TiO_2$, $Tb/TiO_2$ and $[M_4(XW_9O_{34})_2]^{10-}$ ($M = Cu^{2+}$, $Zn^{2+}$, $X = P^{5+}$, $As^{5+}$) (Table 3, entries 1–3). No product was obtained by using of homogeneous sandwich-type polyoxometalate $[Mn_4(GeW_9O_{34})_2]^{12-}$ (Table 1, entry 4). When the same reaction was carried out in the presence of $[Mn_4(XW_9O_{34})_2]^{10-}/Tb/TiO_2$ ($X = P^{5+}$, $As^{5+}$), benzaldehyde was produced with 100% yield (Table 3, entries 5 and 6). Whereas employing $[Zn_4(PW_9O_{34})_2]^{10-}/Tb/TiO_2$ as catalyst the desired product was obtained in less than 70% yield (Table 3, entry 7). Other sandwich-type polyoxometalates such as $[Mn_4(GeW_9O_{34})_2]^{12-}/Tb/TiO_2$ are not effective and do not show any catalytic activity (Table 3, entry 8). These results indicate that manganese ion in $[Mn_4(XW_9O_{34})_2]^{10-}$ ($X = P^{5+}$, $As^{5+}$) with loading on $Tb/TiO_2$ plays significant catalytic role in oxidation of various substrates with hydrogen peroxide.

Finally, in order to extend the scope, oxidation of several alcohols with hydrogen peroxide were investgated in the presence of $[Mn_4(PW_9O_{34})_2]^{10-}/Tb/TiO_2$ as catalyst in water at 80 °C. The expected products were obtained with high yields in short times (Table 4). As shown in Table 4, various types of primary benzylic alcohols, including those with both electron-withdrawing and electron-donating groups, were selectively converted to the corresponding carbonyl compounds in excellent yields (Table 4, entries 1–3). The primary benzylic alcohols with electron-with drawing groups show less reactivity and the oxidation of them require longer reaction times (Table 4, entries 1–3). Benzhydrol and 1-phenylethanol as model for secondary benzylic alcohols were converted to the corresponding carbonyl compounds as well (Table 4, entries 4 and 5). Comparison between our obtained results with the best of the well-known catalytic systems on the oxidation of methyl phenyl sulphide and benzyl alcohol with $H_2O_2$ as oxidant have been given in Tables 5 and 6 (details given in the Supporting Information).

### 4.3 Reactions Mechanism

In the studied the catalytic oxidation system with hydrogen peroxide as oxidant usually two homolytic and heterolytic

**Table 3** Investigate effect of catalysts on the oxidation of benzyl alcohol (1 mmol) to benzaldehyde using $H_2O_2$ (6 mmol) in $H_2O$ (1 mL) at 80 °C

| Entry | Catalyst 20% (40 mg) | Time (h) | Benzaldeyde (%)[a] |
|---|---|---|---|
| 1 | Catalyst-free | 28 | 40 |
| 2 | $Tb/TiO_2$ | 28 | 10 |
| 3 | $[M_4(XW_9O_{34})_2]^{10-}$ M = Mn, Cu, Zn; X = P, As | 15 | 30 |
| 4 | $[M_4(XW_9O_{34})_2]^{12-}$ M = Mn, Cu, Zn; X = Ge | 15 | – |
| 5 | $[Mn_4(PW_9O_{34})_2]^{10-}/Tb/TiO_2$ (10%) | 5 | 100 |
| 6 | $[Mn_4(AsW_9O_{34})_2]^{10-}/Tb/TiO_2$ (10%) | 5 | 100 |
| 7 | $[Zn_4(PW_9O_{34})_2]^{10-}/Tb/TiO_2$ (10%) | 5 | 70 |
| 8 | $[Mn_4(GeW_9O_{34})_2]^{12-}/Tb/TiO_2$ (10%) | 10 | 20 |

[a]Conversions determined by GC

**Table 4** Selective oxidation of alcohols using $H_2O_2$ catalyzed by $[Mn_4(PW_9O_{34})_2]^{10-}$/Tb/$TiO_2$ (10%) in $H_2O$

| Entry | Substrate | Time (h) | Yield (%) |
|---|---|---|---|
| 1 | 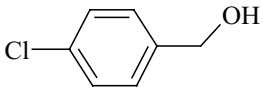 | 5 | 90 |
| 2 | 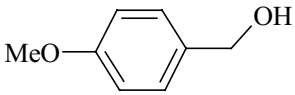 | 1 | 100 |
| 3 | 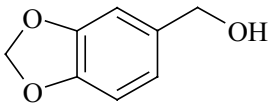 | 4 | 95 |
| 4 | 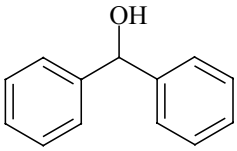 | 4 | 90 |
| 5 | 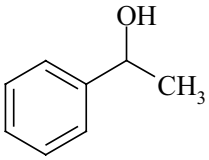 | 5 | 90 |
| 6 | 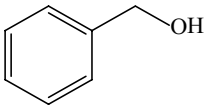 | 5 | 100 |

cleavage of the O–O bond have been reported [67]. In order to study the reaction mechanism of oxidation of alcohols and sulfides catalyzed by $[Mn_4(PW_9O_{34})_2]^{10-}$/Tb/$TiO_2$ and $[Mn_4(AsW_9O_{34})_2]^{10-}$/Tb/$TiO_2$ in the presence hydrogen peroxide as oxidant, 2,2′-Azobis(isobutyronitrile) as radical scavenger was added. The results confirmed that addition of 2,2′-Azobis(isobutyronitrile) has no significant effect on the yield of the product or reaction times. On the basis of above result, we can conclude a heterolytic cleavage of the O–O bond for hydrogen peroxide in this work. Although, the actual role of $[Mn_4(AsW_9O_{34})_2]^{10-}$/Tb/$TiO_2$ is not clear, however on the basis of previously reported mechanism, we can suggest the reaction mechanism as: firstly, hydrogen peroxide reacts with the immobilized polyoxometalate to form the active POM form (peroxo species) which subsequently oxidizes the substrate molecule to yield the product through the heterolytic cleavage of the O–O bond [49, 68–74]. According to the suggested mechanism, the role of hetero atoms in POMs (P or As) can be explained. More active peroxo species were formed with more electronegative hetero atom which followed by complete oxidation of substrate molecule.

### 4.4 Catalyst Recovery and Reuse

The catalyst recovery and reusability are the two most important features for many catalytic processes. The reusability of $[Mn_4(PW_9O_{34})_2]^{10-}$/Tb/$TiO_2$, was investigated for oxidation of benzyl alcohol and methyl phenyl sulfide as a model substrate using $H_2O_2$. In both cases, after the completion of the reaction, the catalyst was easily separated from the reaction mixture by centrifuge, washed with $H_2O$ and dichloromethane to remove the residual product and reused for subsequent experiments under similar reaction conditions. As shown in Fig. 7 the catalyst was reused at least five times with little loss of activity.

The FT-IR spectra of $[Mn_4(PW_9O_{34})_2]^{10-}$/Tb/$TiO_2$ nanocomposite with 10 and 20% loading of POM after five consecutive runs shows that the nanocomposite preserves its fundamental structure. We can expect the catalyst without significant structural changes show the activity in comparison to activity of catalyst in the first run. The FT-IR spectra of $[Mn_4(PW_9O_{34})_2]^{10-}$/Tb/$TiO_2$ after five consecutive runs has been added to the supporting information (Fig. S2).

EDX analysis of $[Mn_4(PW_9O_{34})_2]^{10-}$/Tb/$TiO_2$ and $[Mn_4(PW_9O_{34})_2]^{10-}$/Tb/$TiO_2$ with 10% loading of POMs on Tb/$TiO_2$ after five consecutive runs detect the presence of Mn, O, P, Tb, W and Mn, O, As, Tb, W elements

**Table 5** Comparison of the activity of various catalyst with $[Mn_4(AsW_9O_{34})_2]^{10-}$/Tb/$TiO_2$ and $[Mn_4(PW_9O_{34})_2]^{10-}$/Tb/$TiO_2$ on the oxidation of methyl phenyl sulfide with $H_2O_2$ as oxidant

| Entry | Catalyst | Condition | $H_2O_2$ (mmol) | Time (min) | Conversion (%) sulfoxide/sulfone | References |
|---|---|---|---|---|---|---|
| 1 | $[Mn_4(AsW_9O_{34})_2]^{10-}$/Tb/$TiO_2$(10%) | $CH_3CN$. r.t | 6 | 2 | 100/– | –[a] |
| 2 | $[Mn_4(PW_9O_{34})_2]^{10-}$/Tb/$TiO_2$(10%) | $CH_3CN$. r.t | 6 | 2 | –/100 | –[a] |
| 3 | $[\gamma\text{-}PW_{10}O_{38}V_2(\mu\text{-}OH)_2]^{3-}$ | $CH_3CN$/t-BuOH. 20 °C | 1 | 30 | 98/2 | [36] |
| 4 | $(PyH)H_3PMo_{11}VO_{40}$ | $CH_3CN$. 40 °C | 2–20 | 30 | 100/– | [16] |
| 5 | $H_3PMo_{12}O_{40}$ | $CH_3CN$. 70 °C | 20 | 60 | 88/11 | [37] |
| 6 | $[(C_{18}H_{37})_2(CH_3)_2N]_7\ PW_{11}O_{39}$ | 1,4-Dioxane. 60 °C | 1 | 30 | –/99 | [39] |
| 7 | $TBA_{10}[Fe_4(PW_9O_{34})_2]$ | $CH_3CN$. 50 °C | 2.5 | 60 | –/99 | [60] |

[a]Reaction conditions as exemplified in the experimental procedure

**Table 6** Comparison of the activity of various catalyst with $[Mn_4(PW_9O_{34})_2]^{10-}/Tb/TiO_2$ on the oxidation of benzyl alcohol (1 mmol) to benzaldehyde using $H_2O_2$ as oxidant

| Entry | Catalyst | T(°C)/solvent | Time (h) | Benzaldeyde (%) | References |
|---|---|---|---|---|---|
| 1 | $[Mn_4(PW_9O_{34})_2]^{10-}/Tb/TiO_2$ | 80/$H_2O$ | 5 | 100 | –[a] |
| 2 | $H_3PMo_{12}O_{40}$ | 70/solvent free | 5 | 84 | [43] |
| 3 | $H_3PW_{12}O_{40}$-$NH_2$-IL-SBA-15 | 100/$H_2O$ | 6 | 71 | [51] |
| 4 | $[PMo_{10}V_2O_{40}]^{5-}$SBA-15 | 100/$CH_3CN$ | 12 | 98 | [52] |
| 5 | $SiW_{11}Zn$ | 90/$H_20$ | 9 | 100 | [53] |
| 6 | 1-POM(Zn) | Reflux/$CH_3CN$ | 4.5 | 100 | [67] |

[a]Reaction conditions as exemplified in the experimental procedure

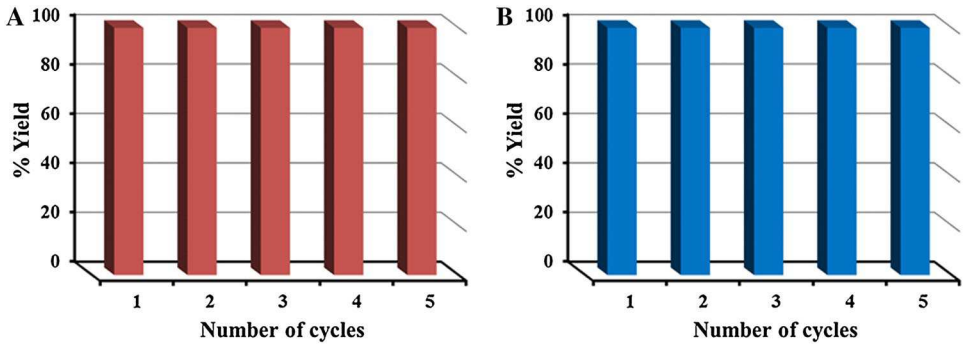


**Fig. 7** The recycling experiment of $[Mn_4(PW_9O_{34})_2]^{10-}/Tb/TiO_2$ for **a** oxidation of methyl phenyl sulfide (1 mmol) to methyl phenyl sulfone using $H_2O_2$ in CH3CN at room temperature and **b** oxidation of benzyl alcohol (1 mmol) to benzaldehyde using $H_2O_2$ (6 mmol) in $H_2O$ at 80 °C

respectively (Fig. S3). Analysis shows that unchanged structure of synthesis nanocomposites after five consecutive runs.

## 5 Conclusions

In this study, we report $[Mn_4(XW_9O_{34})_2]^{10-}/Tb/TiO_2$ ($X = P^{5+}$, $As^{5+}$) nanocomposites as novel immobilized sandwich-type polyoxometalates using surface modified. The structures of synthesized catalysts were confirmed by XRD, FT-IR, TGA, EDX and SEM techniques. We have found that these nanocomposites efficiently catalyze the oxidation of sulfides and benzylic alcohols using $H_2O_2$ as oxidant. The results are summarized as following: (1) the immobilized POMs heterogeneous catalysts could be easily recovered by centrifuge and reused at least five times without significant loss of activity. (2) The oxidant is cheap, green oxidant and easily available. (3) The reactions rate of heterogeneous catalysts are more than the homogeneous catalysts. (4) Selectivity of the reactions increases with the doping of Tb in $TiO_2$. (5) Selectivity and efficiency of nanocomposites include manganese higher than nanocomposites include copper and zinc. (6) In sulfides reaction depending on the type heteroatom in the catalysts different products are created.

**Acknowledgements** The authors would like to thank the University of Kurdistan Research Council for their support of this work.

## References

1. Hill CL (ed) (1998) Special issue on “polyoxometalates”. Chem Rev 98:1
2. Maradur SP, Halligudi SB, Gokavi GS (2004) Catal Lett 96:165
3. Tahar A, Benadji S, Mazari T, Dermeche L, Marchal Roch C, Rabia C (2015) Catal Lett 145:569
4. Egusquiza MG, Cabello CI, Botto IL, Thomas HJ, Casuscelli S, Herrero E, Gazzoli D (2012) Catal Commun 26:117
5. Patel A, Patel K (2014) Inorg Chim Acta 419:130
6. Nardello V, Aubry JM, Vos DED, Neumann R, Adam W, Zhang R, ten Elshof JE, Witte PT, Alsters PL (2006) J Mol Catal A Chem 251:185
7. Santos ICMS, Gamelas JAF, Balula MSS, Simoes MMQ, Neves MGPMS, Cavaleiro JAS, Cavaleiro AMV (2007) J Mol Catal A Chem 262:41
8. Zhao S, Chen Y, Song YF (2014) Appl Catal A General 475:140
9. Yan XM, Lei JM, Liu D, Wu YC, Liu YC, Liu W (2007) Mater Res Bull 42:1905
10. Li D, Guo Y, Hu C, Jiang C, Wang E (2004) J Mol Catal A Chem 207:183
11. Dubey N, Rayalu SS, Labhsetwar NK, Devotta S (2008) Int J Hydrogen Energy 33:5958
12. Alibeik MA, Zaghaghi Z, Baltork IM (2008) Chin J Chem Soc 55:1
13. Itoh H, Utamapanya S, Stark JV, Klabunde KJ, Schlup JR (1993) Chem Mater 5:71
14. Guzman J, Gates BC (2001) Nano Lett 1:689
15. Choudary BM, Kantam ML, Ranganath KVS, Mahender K, Sreedhar B (2004) J Am Chem Soc 126:3396
16. Madesclaire M (1986) Tetrahedron 42:5459
17. Fox A, Dulay MT (1993) Chem Rev 93:341
18. Anandan S, Vinu A, Venkatachalam N, Arabindoo B, Murugesan V (2006) J Mol Catal A Chem 256:312

19. Hoffman MR, Martin ST, Choi W, Bahnemann DW (1995) Chem Rev 95:69
20. Okuhara T, Mizuno N, Misono M (1996) Adv Catal 41:113
21. Neumann R (1998) Prog Inorg Chem 47:317
22. Kozhevnikov IV (2002) Catalysts for fine chemical synthesis catalysis by polyoxometalates. Wiley, Chichester
23. Hill CL (2004) Polyoxometalates: reactivity. In: McCleverty JA, Meyer TJ (eds) Comprehensive coordination chemistry, vol II. Elsevier Pergamon, Amsterdam, pp 4
24. Mizuno N, Kamata K, Uchida S, Yamaguchi K (2009) In: Mizuno N (ed) Modern heterogeneous oxidation catalysis: design, reactions and characterization. Wiley-VCH, Weinheim
25. Strukul G (1992) Catalytic oxidation with hydrogen peroxide as oxidant (Kluwer). Springer, Dordrecht
26. Shiozaki R, Goto H, Kera Y (1993) Bull Chem Soc Jpn 66:2790
27. Griffith WP, Moreea RGH, Nogueira HIS (1996) Polyhedron 15:3493
28. Shiozaki R, lnagaki A, Ozaki A, Kominami H, Yamaguchi S, Ichihara J, Kera Y (1997) J Alloys Compd 261:132
29. Siozaki R, Inagaki A, Kominami H, Yamaguchi S, Ichihara J, Kera Y (1997) J Mol Catal A 124:29
30. Gresley NM, Griffith WP, Laemmel AC, Nogueria HIS, Parkin BC (1997) J Mol Catal A 117:185
31. Griffith WP, Morley-Smith N, Nogueria HIS, Shoair AGF, Suriaatmaja M, White AJP, Williams DJ (2000) J Organomet Chem 607:146
32. Prilezhaeva EN (2001) Russ Chem Rev 70:897
33. Prilezhaeva EN (2000) Russ Chem Rev 69:367
34. Rich DH, Tam JP (1977) J Org Chem 42:3815
35. Burrage S, Raynham T, Williams G, Essex JW, Allen C, Cardno A, Swali V, Bradley M (2000) Chem Eur J 6:1455
36. Padwa A, Danca MD (2002) Org Lett 4:715
37. Procter DJ (2000) J Chem Soc Perkin Trans 1:835
38. Gresley NM, Griffith WP, Laemmel AC, Nogueira HIS, Parkin BC (1997) J Mol Catal 117:185
39. Collins FM, Lucy AR, Sharp C (1997) J Mol Catal 117:397
40. Zhao S, Jia Y, Song YF (2013) Appl Catal A General 453:188
41. Yamaura T, Kamata K, Yamaguchi K, Mizuno N (2013) Catal Today 203:76
42. Romanelli GP, Paula IV, Caceres CV, Vazquez PG, Tundo P (2011) Catal Commun 12:726
43. Tundo P, Romanelli GP, Vazquez PG, Arico F (2010) Catal Commun 11:1181
44. Rahimizadeha M, Rajabzadehb G, Khatamia SM, Eshghia H, Shiri A (2010) J Mol Catal A Chem 323:59
45. Xue X, Zhao W, Ma B, Ding Y (2012) Catal Commun 29:73
46. Tojo G, Fernández M (2006) Oxidation of alcohols to aldehydes and ketones (1st edn). Springer, New York
47. Centi G, Cavani F, Trifiro F (2001) Selective oxidation by heterogeneous catalysis (1st edn). Kluwer Academic Publishers, New York
48. Venturelo C, Gambero M (1991) J Org Chem 56:5924
49. Zhao W, Zhang Y, Ma B, Ding Y, Qiu W (2010) Catal Commun 11:527
50. Ma B, Zhang Y, Ding Y, Zhao W (2010) Catal Commun 11:853
51. Tan R, Liu C, Feng N, Xiao J, Zheng W, Zheng A, Yin D (2012) Microporous Mesoporous Mater 158:77
52. Bordoloi A, Sahoo S, Lefebvre F, Halligudi SB (2008) J Catal 259:232
53. Wang J, Yan L, Li G, Wang X, Dinga Y, Suoa J (2005) Tetrahedron Lett 46:7023
54. Bonadies F, Angelis FD, Locati L, Scettri A (1996) Tetrahedron Lett 37:7129
55. Kaczorowska K, Kolarska Z, Mitka K, Kowalski P (2005) Tetrahedron 61:8315
56. Finke RG, Droege M (1981) J Am Chem Soc 103:1587
57. Kortz U, Nellutla S, Stowe AC, Dalal NS, Rauwald U, Danquah W, Ravot D (2004) Inorg Chem 43:2308
58. Yajun W, Kecheng L, Changgen F (2011) J Rare Earths 29:866
59. Lv K, Xu Y (2006) J Phys Chem B 110:6204
60. Gomez-Garcia CJ, Coronado E, Gomez-Romero P, Casan-Pastor N (1993) Inorg Chem 32:3378
61. He NY, Woo CS, Kim HG, Lee HI (2005) Appl Catal A 281:167
62. Siahkali AG, Philippou A, Dwyer J, Anderson MW (2000) Appl Catal A 192:57
63. Salvati L, Makovsky LE, Stencel JM, Brown FR, Hercules DM (1981) J Phys Chem 85:3700
64. Moulder JF, Stickle WF, Sobol PE, Bomben KD (1992) Handbook of X-ray photoelectron spectroscopy. Perkin-Elmer, Eden Prairie
65. Sato K, Aoki M, Noyori R (1998) Science 281:1646
66. Sato K, Hyodo M, Aoki M, Zheng XQ, Noyori R (2001) Tetrahedron 57:2469
67. Neumann R, Gara M (1994) J Am Chem Soc 116:5509
68. Haddadi H, Riahi Farsani M (2015) J Clust Sci. doi:10.1007/s10876-015-0936-0
69. Duncan DC, Chambers RC, Hecht E, Hill CL (1995) J Am Soc Chem 117:681
70. Grecley NM, Griffith WP, Laemmel AC, Nogueira HS, Parkin BC (1997) J Mol Catal 117:185
71. Gao J, Chen Y, Han B, Feng Z, Li C, Zhou N, Gao S, Xi Z (2004) J Mol Catal A Chem 210:197
72. Ding Y, Zhao W, Hua H, Ma BC (2008) Green Chem 10:910
73. Zhao W, Ma B, Hua H, Zhang Y, Ding Y (2008) Catal Commun 9:2455
74. Zhang Z, Zhao W, Ma B, Ding Y (2010) Catal Commun 12:318